# Probabilistic Day-ahead Inertia Forecasting

Evelyn Heylen, Jethro Browell, *Senior Member, IEEE,*, Fei Teng, *Senior Member, IEEE,*

***Abstract*—Power system inertia is declining and is increasingly variable and uncertain in regions where the penetration of non-synchronous generation and interconnectors is growing. This presents a challenge to power system operators who must take appropriate actions to ensure the stability and security of power systems relying on short-term forecasts of the system's inertial response. Existing models to forecast inertia fail to quantify uncertainty, which may prevent their utilization given the risk aversion of the system operators when handling stability issues. This paper is the first to develop a model to produce calibrated, data-driven probabilistic forecasts of the inertia contribution of transmission-connected synchronous generators. The model provides a necessary tool for system operators to quantify forecast uncertainty, allowing them to manage the risk of frequency instability cost-effectively. The paper demonstrates that the assumption of a Gaussian distribution of uncertainty applied in existing models is not acceptable to accurately forecast the inertial response and provides a satisfactory forecast model by combining non-parametric density forecasting with parametric tail distributions. Moreover, the paper shows that satisfactory predictive performance can only be achieved by adopting a rolling horizon forecast approach to deal with the rapidly changing characteristics of the inertial response in power systems.**

***Index Terms*—Inertia forecasting, probabilistic forecasting, energy forecasting, frequency response**

## I. Introduction

Driven by the integration of power-electronic-interfaced generation, load and interconnections, the declining level of inertial response in power systems and its changing characteristics challenge system operators in maintaining system stability and efficiently operating the system. On the one hand, system operators change the dispatch to keep the rate of change of frequency (ROCOF) within limits by increasing the inertia or reducing the largest loss in the system. On the other hand, frequency containment reserves and fast frequency reserves, such as dynamic containment (Great Britain) or fast frequency reserve (Nordic area), are scheduled to keep the frequency nadir within limits following the largest loss of infeed or offtake. However, the dimensioning of the required volumes critically depends on system inertia conditions [1], [2] and should be done ahead of real time. Therefore, the cost-effectiveness of the actions and the resulting security of the system relies upon accurate forecasts of system inertia.

However, forecasting the level of inertial response is extremely challenging as it depends on multiple factors, such as generation from weather-dependent non-synchronous sources, load, generator failures, market forces and strategic behaviour of generators [3]. In fact, inertia forecasting is a much less explored topic compared to related issues, such as load and wind power forecasting. The first paper in this field was published by Du and Matevosyan in 2018 [4], focusing on the inertia contribution of transmission-system-connected synchronous generator units. This forecast model relies upon a physical model of synchronous generators' contribution to inertia using the expected synchronized status of each individual generator resulting from a centralized unit commitment. Follow-up research on inertia forecasting has relied upon the same model, but added a linear regression model that expresses the contribution of embedded units as a function of the demand forecast [5]. A major concern of the physical-model-based forecast is the availability and accuracy of forecast synchronized status of each individual generator [6]. The independent system operator ERCOT has indicated the risk of inaccurate forecasts of the individual generators' real-time status resulting in overcasts of the inertia, especially during low-price periods [4]. This effect is even more significant in power systems with independent market operators that typically do not have control over the unit commitment. Moreover, the uncertainty on the synchronized status of individual generators will only increase with the increasing amount of renewable energy sources. To this end, time-series forecast models based on historic values of the inertial response of transmission-connected synchronous generators are developed, which do not explicitly depend on the forecast online status of individual generators [7]. However, existing models only provide point forecasts of expected inertia to the system operator [4], i.e., forecasts of the expected value of the inertia level, or the forecast models assume a Gaussian distribution of the residuals with constant variance [7], which may be violated in practice.

Point forecasts and their related Gaussian assumptions of uncertainty are unsatisfactory to ensure cost-effectiveness of current and future system operation. Given the extreme costs of power interruptions, system operators must rely upon the extreme quantiles of the predictive distribution. This requires accurate modelling of the complete distribution of the real-time inertia, while special attention for accurate modelling of the tails is critical [8], [9].[1] Although an extensive literature exists on probabilistic forecasting of related variables, such as wind power, demand and electricity prices [11], insights into the day-ahead (D-1) predictive distribution of inertia from transmission-connected synchronous generators are still missing.

To the best of the authors' knowledge, this is the first paper to study the characteristics of the predictive distribution of system inertia. In this context, the paper focuses on the range of explanatory variables available to forecast the inertia contribution of transmission-connected synchronous generators. To get insight into the characteristics of the D-1 predictive distribution of inertia from transmission-connected

Evelyn Heylen and Fei Teng are with the Department of Electrical and Electronic Engineering, Imperial College London, London, UK. Jethro Browell is with the University of Glasgow. Corresponding Author: Dr Fei Teng (f.teng@imperial.ac.uk)

[1]The authors have work in preparation, specifically focusing on the use of probabilistic inertia forecasts in system operation.

synchronous generators in power systems, we have applied statistical estimation techniques to a data set of estimated inertia data as well as data of multiple exogenous variables from Great Britain. The paper informs system operators on how they can improve their existing inertia forecasting practice by accurately considering the uncertainty related to the D-1 forecasts with a probabilistic forecast model, as well as hints for dealing with the long-term evolution of their system that affects the overall inertia level. This paper provides the first benchmark model for probabilistic forecast models of inertia from transmission-connected synchronous generators. The data set used to build the model is publicly available for validating the results and for benchmarking improved or adapted forecast models.

Section II elaborates on the inertia contribution of transmission-connected synchronous generators. Section III explains the theory of the probabilistic forecast models, including the methodology to evaluate the predictive accuracy and calibration of the probabilistic models. Section IV elaborates on the development of the probabilistic model to forecast the inertia of transmission-connected synchronous generators for the Great Britain data. It gives insight into the important features to be considered in the forecast model. Section V evaluates and validates the model on unseen test data and elaborates on ways to make the forecast models robust against the evolutions in power systems. Section VI concludes the paper.

## II. Transmission-connected synchronous generators inertia contribution

Inertial response is defined as the resistance in the form of energy exchange to counteract the changes in system frequency resulting from power imbalances in generation and demand [12]. Therefore, inertia is a crucial asset in power systems to keep the system stable and avoid disconnection of loads. The inertial response available in real time should be sufficient to keep the ROCOF within limits and limit the largest frequency deviation in combination with adequately procured frequency response services.

Today, the main source of inertial response is the kinetic energy of rotating masses that are directly connected to the system and synchronized with the system frequency. These rotating masses can instantaneously convert rotating kinetic energy into electrical energy (or the reverse) to oppose an imbalance between demand and supply in the system, and as a result changing their rotational speed and thus system frequency.[2] Transmission-connected synchronous generator units are an important contributor to the inertial response from synchronized rotating masses available in the system. The inertia contribution of transmission-connected synchronous generator units depends upon the individual generators' online status according to physical model

$$E_t^{I,G} = \sum_i H_i \cdot P_i^{G,C} \cdot K_{i,t} \qquad [MVAs] \tag{1}$$

[2]Convertor-interfaced energy sources, such as modern wind turbines or storage units, may provide virtual inertia with adequate control strategies, but this contribution has not been widespread in the system of today yet.

where $P_i^{G,C}$ represents the generation capacity of each individual generator $i$, which is well-known to the system operator. $H_i$ represents the inertia constant per individual generator. $K_{i,t}$ represents the status of generator $i$ at time instant $t$, i.e., whether it is synchronized to the system or not. Without any control action of the system operator, such as generator startup actions, the status of a generator depends upon the outcomes of the energy markets, e.g., day-ahead and intraday markets. The market clearing and resulting generator statuses are determined by the bids of the different generators to sell their energy combined with the expected demand for electrical energy.

While historically generator statuses were quite predictable given the predictability of the demand pattern and the controllability of synchronous generator units, this is no longer the case. Today, the market clearing is impacted by forecasts of uncertain renewable generation units, such as wind and solar. These forecasts determine the net system demand and the volume of the bids from renewable generation units, which will always be in the market due to their low marginal cost. Demand that cannot be supplied by variable renewable energy sources needs to be met by synchronous generator units and/or imported from other countries via interconnectors. The expected generator statuses may continuously change from day ahead up to real time due to bilateral trading and trading on the intraday energy markets for balancing demand and supply considering changing forecasts of demand and renewable generation. This probabilistic character of power systems causes that a single set of day-ahead forecast values of demand and renewable power generation can result in different real-time realizations of the inertial response of transmission-connected synchronous generators available in the system. To reduce the risk of load shedding and ensure the cost-effectiveness of system operation, probabilistic forecasts should accurately capture the uncertainty associated with the predictions of inertial response at any given point in the future.

## III. Probabilistic forecast model: Theory

A probabilistic forecast aims to predict and describe the uncertainty associated with a given target variable. Forecasts are made at time $t$ for some time $t + k$ in the future, defined by the predictive distribution $\hat{F}_{t+k|t}(E_{t+k}^{I,G}; \boldsymbol{x}_t)$. The predictive distribution quantifies forecast uncertainty in the form of a probability distribution instead of only focusing on forecasting the expected value. The target variable in this paper is the aggregated inertial response from transmission-connected synchronous generators, as defined in Eq. (1). The forecast horizon is one day. The system state $\boldsymbol{x}_t$ at the time a forecast is produced can be represented by a vector with the values of exogenous variables available at that time, i.e., one day ahead of real time, as its elements. Considered exogenous variables are for instance the D-1 wind forecast, solar forecast, demand forecast, etc.

Different structures to model the conditional distribution exist, which may be parametric, semi-parametric or non-parametric in nature. Probabilistic forecasting of energy variables is an active field of study [13] spanning wind [14], load

[15] and electricity prices [16]. This provides a rich literature of forecasting models that incorporate energy-domain knowledge which we draw upon here [17]. In this paper, we worked in the generalized additive modelling framework to develop a new type of probabilistic forecast model, i.e., a model to forecast the inertia contribution of transmission-connected synchronous generators. We present and compare a Gaussian parametric probabilistic model, non-parametric quantile regression models and a hybrid model combining non-parametric quantile regression with parametric modelling of the tails of the distribution for day-ahead inertia forecasting.

### A. Parametric predictive distribution

By assuming that the predictive distribution of the quantity being forecast follows a parametric form, the prediction task is reduced to forecasting the distribution's parameter values. In the case of the Gaussian distribution, this is the mean and standard deviation. We follow this approach here as a benchmark, and write the predictive distribution as

$$\hat{F}_{t+k|t}(E^{I,G}_{t+k};\boldsymbol{x}_t) = \Phi(E^{I,G}_{t+k};\hat{\mu}_{t+k|t},\hat{\sigma}) \tag{2}$$

where $\Phi(\cdot)$ is the Gaussian distribution. The conditional mean $\hat{\mu}_{t+k|t}$ is estimated as $\hat{E}^{I,G}_{t+k|t}$, which may be considered a deterministic forecast, and linear models for the conditional mean are simple to estimate and discussed later in this section. We assume the standard deviation of the predictive distribution $\hat{\sigma}^2$ is constant and estimate it using the sample standard deviation from training data.

### B. Non-parametric predictive distribution

Parametric distributions have a fixed shape and limited flexibility, which may not be a good representation of reality, resulting in poor forecast performance. A non-parametric predictive distribution can be constructed in a piece-wise fashion by estimating a series of predicted quantiles via quantile regression [18]. In this case, a separate model is required for each quantile $\hat{q}^{(\tau)}_{t+k|t}$ at a range of probability levels $\tau_L \leq \tau \leq \tau_R$. A continuous predictive distribution $\hat{F}_{\text{QR}}(E^{I,G}_{t+k};\boldsymbol{x}_t)$ may be formed by interpolating between quantiles, and extrapolating beyond $\hat{q}_{\tau_L}$ and $\hat{q}_{\tau_R}$. Linear models with the same structure as for $\hat{E}^{I,G}_{t+k|t}$ may be estimated to predict conditional quantiles, though this can be computationally more demanding than modelling the conditional expectation.

### C. Parametric tail distributions

In the tails of the predictive distribution, quantiles with probabilities close to 0 and 1, estimating quantile regression models becomes challenging due to the limited availability of data, by the very nature of the problem. We therefore consider a parametric distribution for the tails in order to produce full predictive distributions while retaining the flexibility of quantile regression for non-extreme probability levels. Extreme value theory provides a theoretical basis for this, specifically the Generalized Pareto Distribution (GPD), which describes the distribution of 'peaks over a threshold'. The GPD $F_{\text{GPD}}(\cdot)$ is characterized by scale and shape parameters $\nu$ and $\xi$, respectively [19], and may be conditioned on explanatory variables for increased flexibility if required [8]. The resulting semi-parametric predictive distribution $\hat{F}_{\text{S}}(E^{I,G}_{t+k})$ is given by

$$\begin{cases} \tau_L F_{\text{GPD}}(\hat{q}_{\tau_L} - E^{I,G}_{t+k};\nu_L,\xi_L) & \text{for } E^{I,G}_{t+k} < \hat{q}_{\tau_L}, \\ \hat{F}_{\text{QR}}(E^{I,G}_{t+k};\boldsymbol{x}_t) & \text{for } \hat{q}_{\tau_L} \leq E^{I,G}_{t+k} \leq \hat{q}_{\tau_R}, \\ \tau_R + (1-\tau_R)F_{\text{GPD}}(\hat{q}_{\tau_R} + E^{I,G}_{t+k};\nu_R,\xi_R) & \text{for } E^{I,G}_{t+k} > \hat{q}_{\tau_R}. \end{cases} \tag{3}$$

### D. Benchmarking

As this is the first paper to develop a probabilistic inertia forecast model, sophisticated benchmark models do not exist yet. For this reason, the forecast models have been benchmarked against two autoregressive-type models. The autoregressive models have the following model structures

$$\begin{aligned} \hat{E}^{I,G}_{t+k|t} = \; & a_1 E^{I,G}_{t+k-48} + b_1 s_1(E^{I,G}_{t+k-48}) + \\ & a_2 E^{I,G}_{t+k-336} + b_2 s_2(E^{I,G}_{t+k-336}) \end{aligned} \tag{4}$$

where $s_i(\cdot)$ are smooth terms able to capture non-linear responses. The first autoregressive model (AR48) is a linear regression of the inertial response at the instant of forecasting (i.e., $a_2 = 0$ and $b_2 = 0$), whereas the second autoregressive model (AR336) additionally considers the inertial response in the system one week or 336 settlement periods of 30 minutes before the time instant of interest. The order of the autoregressive models has been chosen based on inspection of partial autocorrelation plots. The autoregressive models have a generalized additive model structure with a linear term and a smoothing spline term with a thin plate regression spline as smoothing basis per variable [20]. This elaboration of classical autoregressive models was chosen after observing a non-linear autoregressive relationship during data exploration.

On top of this, the proposed forecast models have been benchmarked against a more complex, non-linear multilayer perceptron (MLP) machine learning model. The MLP model has the same features as the best-performing proposed model. Hyperparameter tuning resulted in a MLP model with three hidden layers with 20 nodes per layers, sigmoid activation functions and trained using the ADAM solver.

### E. Evaluation

The developed forecast models are evaluated using a range of established metrics to assess their performance. Point forecasts are evaluated using Root Mean Squared Error (RMSE), Mean Absolute Percentage Error (MAPE) and Mean Overestimation Percentage Error (MOPE). Probabilistic forecasts have their calibration verified and are evaluated using Continuous Ranked Probability Score.

The calibration of a probabilistic forecast measures the statistical consistency between the predictive distributions and the observations, which is a joint property of the forecasts and the observations [21]. The calibration is assessed in this paper using a histogram of the probability integral transform (PIT). The PIT is defined as $u_t = \hat{F}_t(E^{I,G}_t)$, with $E^{I,G}_t$ the observations of the inertial energy in the system and $\hat{F}_t(.)$ the derived predictive cumulative distribution function for a

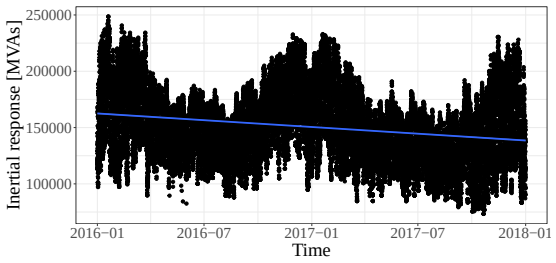


Fig. 1: Evolution of the inertial response from transmission-connected synchronous generators in 2016 and 2017 with the decreasing trend indicated in blue.

given time instant following from the developed probabilistic forecast model [22]. This results in a random variable $U$, with realizations $\{u_t\}$, that follows a uniform distribution for well calibrated forecasts with a sufficiently large sample. The histogram of the PIT allows to assess the shape of the distribution of $u_t$ and thus the calibration of the probabilistic forecast. A well-calibrated forecast has a constant PIT histogram. To deal with the sample uncertainty of the observations at hand, confidence intervals have been included in the PIT histograms. The confidence intervals are calculated according to the normal approximation of the binomial distribution. The impact of serial correlation is considered in the evaluation of the calibration of the final model on the test data. The confidence intervals become wider if temporal correlation in the data is considered, so if the PIT is within the confidence intervals without serial correlation it automatically is within the confidence intervals with temporal correlation considered. To consider the temporal correlation, a surrogate consistency resampling method that preserves the rank correlation and therefore account for the impact of serial correlation is used [23].

To evaluate and compare the performance of well-calibrated probabilistic forecasts, sharpness and resolution are considered. The CRPS not only accounts for calibration, but also for the sharpness and the resolution of predictive distributions [24]. It is defined in Eq. 14 in [22]. The more concentrated the predictive distributions are, i.e., the sharper, the better, subject to calibration. Sharp forecasts imply that the system operator is subject to less uncertainty on the forecast variable. If different calibrated forecast models have similar sharpness, models with greater resolution, those with larger variation in prediction interval width, are preferred as they have a better ability to discriminate between events.

## IV. Probabilistic inertia forecast model: Development and tuning

Probabilistic models for day-ahead forecast of the available inertia from large transmission-connected generators in the system are developed based on data from the Great Britain electricity transmission system.

### A. Data

To facilitate reproduction of the forecast models developed here, and benchmarking of future model improvements, this paper comes with a public data set. The data set contains data from Great Britain for the years 2016, 2017 and 2018, which are collected from Elexon's BM reports[3], ENTSO-E's data transparency platform[4], National Grid's data explorer[5] and the Nordpool website[6]. The combined data set contains the features summarized in Table I. The data sets from different sources have been made consistent in terms of time zones. Some periods suffering data quality issues have been excluded. Moreover, time instants suffering from unexpected zero forecasts of wind power generation or unexpectedly low online capacity of the transmission-connected synchronous generators are removed from the data set.

TABLE I: Exogenous features available in the public data set

| Feature type | Feature name |
|---|---|
| Demand | transmission system demand (TSD), national demand (ND) |
| Real-time generation capacity | coal, nuclear, combined-cycle gas turbine (CCGT), wind, pumped hydro, hydro, biomass, solar, open-cycle gas turbine (OCGT), total capacity |
| Interconnector flows | France (IFA1), Netherlands (BritNed), Island of Ireland (East-West and Moyle), total interconnection flow |
| Day-ahead forecasts | solar, onshore wind, offshore wind, national demand, transmission system demand |
| Electricity price | hourly electricity price from the day-ahead auction |
| Inertial response | inertial response from coal, nuclear, CCGT, pumped hydro, non-pumped hydro, biomass, OCGT, and total inertial response = **Target variable** |

Based on the data collected from the different sources, the inertia contribution from large transmission-connected synchronous generators has been estimated based on Eq. (1). The online capacity per individual generator has been estimated based on the generation output of each individual transmission-connected synchronous generator unit per time instant in Elexon's BM reports, which determines whether the unit was synchronized with the system, and the capacity per transmission-connected generator unit published in Elexon's BM reports. In practice, the inertia constants of specific generators are known to the system operator, which can be directly used in the forecasting model. However, due to the commercial sensitivity, such data can not be made publicly available. Therefore, we select representative inertia constants based on data available in the literature [25] and sample inertia constants for individual generators from normal distributions that differ per generator type.[7] Table II summarizes the parameters of the normal distributions of the inertia constants per generator type used to calculate the inertial response in the system at each time instant.

[3]https://www.bmreports.com/bmrs/?q=help/about-us[Accessed10/07/2020]
[4]https://transparency.entsoe.eu/ [Accessed 10/07/2020]
[5]https://data.nationalgrideso.com/ [Accessed 10/07/2020]
[6]https://www.nordpoolgroup.com/ [Accessed 10/07/2020]
[7]The mean of the Gaussian distributions of the inertia constants is based on [12] and [25].

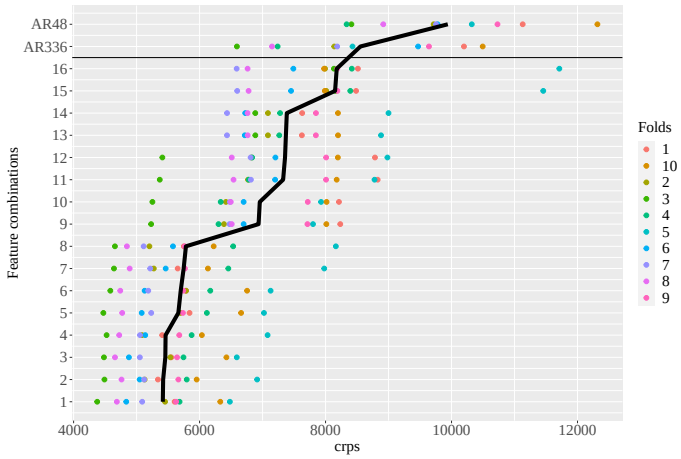


| Model no. | Time | Historical inertia | National Demand forecast | Wind forecast | Solar forecast |
|---|---|---|---|---|---|
| 16 | n | n | y | n | y |
| 15 | n | n | y | n | n |
| 14 | n | y | y | n | y |
| 13 | n | y | y | n | n |
| 12 | y | n | y | n | y |
| 11 | y | n | y | n | n |
| 10 | y | y | y | n | y |
| 9 | y | y | y | n | n |
| 8 | n | n | y | y | n |
| 7 | n | n | y | y | y |
| 6 | y | n | y | y | n |
| 5 | y | n | y | y | y |
| 4 | n | y | y | y | n |
| 3 | y | y | y | y | n |
| 2 | n | y | y | y | y |
| 1 | y | y | y | y | y |

Fig. 2: Learning curve for different degrees of model complexity assuming a Gaussian predictive distribution considering 10-fold cross-validation and the continuous rank probability score as a performance metric evaluated for the training data. The table specifies the variables included in the model structures assessed in the learning curve (y: included, n: not included)

TABLE II: Parameters of the normal distribution of the inertia constants per generator type

| | $\sigma$ [s] | $\mu_g$ [s] |
|---|---|---|
| Coal | 0.6 | 5 |
| Nuclear | 0.85 | 6 |
| Combined-cycle gas turbine | 0.5 | 4 |
| Biomass | 0.5 | 4 |
| Non-pumped storage hydro | 0.9 | 6 |
| Fossil gas | 0.8 | 4 |
| Fossil hard coal | 0.65 | 4 |
| Fossil oil | 0.7 | 4 |
| Hydro-run-of-river and poundage | 1.0 | 6 |
| Open-cycle gas turbine | 0.6 | 4 |
| Other | 0.4 | 4 |

The category 'Other' refers to non-specified generators connected to the transmission system, but not further classified by National Grid. It does not cover demand-response capabilities or grid-forming invertor capabilities at the moment.

To test the performance of the model on out-of-sample data, the data set has been divided in a training set and test set. The data of the years 2016 and 2017 have been considered as training data, whereas the data of 2018 have been considered as test data. Fig. 1 shows the evolution of the inertial response from transmission-connected synchronous generators for the years 2016 and 2017. The profile shows a yearly and daily periodicity as well as a decreasing trend in the inertial energy. The data of 2016 and 2017 have been used to develop the models, whereas the test set is only used during final performance evaluation.

### *B. Modelling of the conditional mean of a parametric Gaussian predictive distribution*

10-fold cross-validation on the training data has been used to select a suitable structure to model the conditional mean of the parametric Gaussian predictive distribution as a function of exogenous variables, temporal variables and lagged versions of the target variable. A linear correlation analysis has shown strong correlation between the inertial response available the next day and the forecast of demand. The model comparison starts from a simple linear model structure with the day-ahead forecast of national demand as a single variable. The national demand is the net load in the system, i.e., the load minus the solar and wind power generation. Additionally, the impact of adding other system variables available in day ahead to the model structure on the predictive accuracy has been assessed. These variables are day-ahead forecasts of wind power generation (onshore and offshore), solar power generation, the inertial energy at the moment of forecasting and temporal variables. Fig. 2 shows the learning curve in terms of the continuous ranked probability score for 10-fold cross-validation considering different linear structures to model the mean of Gaussian predictive distributions. The variance of the Gaussian is assumed to be constant for this analysis. The best performing model in Fig. 2, model no. 1, considers the forecast of wind generation, solar generation, the inertia at the moment of forecasting, as well as the negative trend in the inertia with time (linear and quadratic). The resulting model is given by[8]

$$\hat{E}^{I,G}_{t+k|t} = \alpha_1 E^{I,G}_t + \alpha_2 \hat{P}^{ND}_t + \alpha_3 \hat{P}^{wind}_t + \alpha_4 \hat{P}^{solar}_t + \alpha_5 t + \alpha_6 t^2 \quad (5)$$

The inertial response the next day is expected to be higher if the day-ahead demand forecast and the inertial energy at the time of forecasting are higher (positive coefficients), whereas high forecast values for wind and solar power generation in day-ahead are expected to result in a lower level of inertia the next day (negative coefficients). This is caused by the fact that solar and wind power plants do not provided inertia to the system at present.

The residuals of model no. 1 have been assessed as a function of different covariates. Two covariates that show clear relationships with the residuals are the interconnection flows and whether we are forecasting for a weekday or a holiday / weekend day, as shown in Fig. 3. Especially when

[8]The values of the coefficients are summarized in Table IV in Appendix.

forecasting for holidays/weekend days, there is a higher risk for overestimating the inertia that will be available. The decreasing trend of the residuals with the interconnection flows indicates that if more power is imported into the system (positive interconnection flow), the risk of overestimating the available inertial response is higher (negative residual). This is caused by the convertor-interfaced interconnectors preventing imported power to provide inertia to the system. We have also assessed the impact of explicitly considering seasonality in the model structure, i.e., changing the model coefficients per season. However, this change had only limited impact on the predictive performance and has not been considered further.

To improve the accuracy of the model, we have modified the model structure in model no. 1 (according to Fig. 2 and Eq. (5)) in two ways. First of all, after observing distinct behaviours relating to day-types, we fit separate models for week-days and non-weekdays (including public holidays). Second, introducing the net real-time interconnection flow aggregated for all convertor-interfaced interconnectors as a variable in the model structure has a positive impact. The structure of the model with the impact of the total net interconnection flow $P_t^{ic}$ is given by[9]

$$\begin{aligned}\hat{E}_{t+k|t}^{I,G} = \; & \beta_{1,d} E_t^{I,G} + \beta_{2,d} \hat{P}_t^{ND} + \beta_{3,d} \hat{P}_t^{wind} + \\ & \beta_{4,d} \hat{P}_t^{solar} + \beta_{5,d} P_t^{ic} + \beta_{6,d} \cdot t + \beta_{7,d} \cdot t^2 \end{aligned} \quad (6)$$

and is estimated separately for weekdays and non-weekdays (type of day indicated by subscript d). First of all, the impact of the inertial response level is an order of magnitude smaller when forecasting for a weekend day / holiday compared to a weekday, as the previous (week)day is typically not representative for the weekend day / holiday. Second, positive interconnection flows, corresponding to import to the system, result in a lower inertia level to be expected the next day. As this import is provided by HVDC interconnectors, inertia is no byproduct of the imported energy having a negative impact on the level of inertia in the system.

The resulting performance metrics on the train data are shown in Table III. The improvement in forecast accuracy if the interconnection flow is added as a variable to the model structure indicates the importance of including an accurate forecast of the interconnector flows in the forecast model.[10] Fig. 4 shows that the trends in the residuals have disappeared with the modifications to the model.

In general, the developed models outperform the benchmark autoregressive models in terms of the different performance metrics for the training set, as shown in Table III. All performance metrics have more than halved, both the metrics that are related to the point forecast models as well as the continuous ranked probability score. Moreover, the performance metrics of the proposed forecast models have similar order of magnitudes as and are even slightly better than more complex, non-linear MLP machine learning models with the same features. On top of their improved performance, a clear advantage of the proposed models is their interpretability and explanatory character.

[9]The values of the coefficients are summarized in Table IV in Appendix.

[10]As day-ahead forecasts of the interconnection flows are currently not publicly available, we have used the real-time realization in model development.

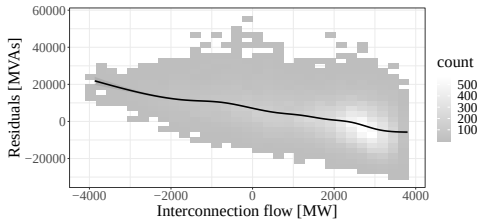


(a) Interconnection flow

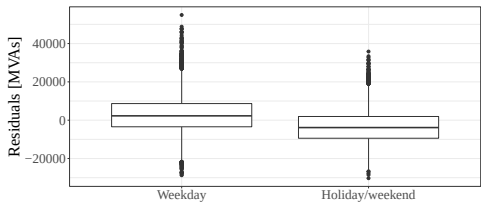


(b) Type of day

Fig. 3: Residuals of model no. 1 in Fig. 2 as a function of the interconnection flow and type of day (weekday or weekend day/holiday). A negative value on the y-axis implies an overcast of the inertial response.

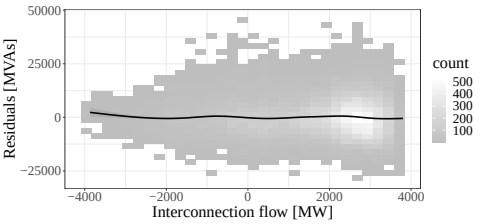


(a) Interconnection flow

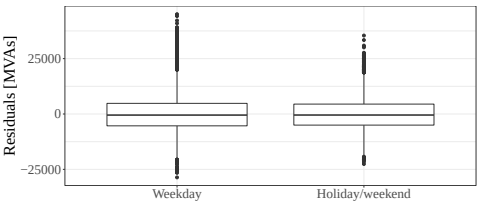


(b) Type of day

Fig. 4: Residuals of the model specified in Eq. (6) as a function of interconnection flow and type of day (weekday or weekend day/holiday).

### C. Calibration of probabilistic forecast models on train data

The calibration of the best-performing parametric Gaussian predictive distribution according to the CRPS in Table III is not acceptable. Fig. 5a shows the histogram of the PIT with 95% confidence intervals and 100 breaks for the model presented in Eq. (6). The PIT histogram in Fig. 5a shows deviations compared to the reference line of the uniform distribution of the PIT, especially in the tails. The histogram also suggests that some skewness in the distribution is not captured by the Gaussian predictive distribution.

TABLE III: Performance metrics on the train data of the benchmark and the developed forecast models

| Model name | RMSE [MVAs] | MAPE [%] | MOPE [%] | CRPS [MVAs] |
|---|---|---|---|---|
| AR48 | 17885 | 9.6 | 10.7 | 9927 |
| AR48_AR336 | 15222 | 8.3 | 9.3 | 8523 |
| Model no. 1 (Eq. (5)) | 9387.5 | 5.1 | 5.3 | 5258 |
| Model no. 1 + IC flow | 8125 | 4.4 | 4.5 | 4536 |
| Model no. 1 + type of day | 8860 | 4.8 | 4.9 | 4949 |
| Model no. 1 + IC flow and type of day (Eq. (6)) | 7733 | 4.2 | 4.2 | 4314 |
| MLP | 10368 | 5.8 | 5.6 | 5847 |

Quantile regression is a non-parametric modelling technique that facilitates to account for the skewness in the distribution [26]. Equidistant quantiles between the 5% and 95% have been modelled (5% distance) as well as the 1% - 5% and 95% - 99% quantiles with 1% distance. Interpolation using a monotone Hermite spline has been applied between the quantiles and linear interpolation with lower bound zero and upper bound one has been applied below and above the 1% and 99% quantile resp. The model structure of the quantiles is the same as in Eq. (6), with different model coefficients per quantile. The quantile regression model is calibrated better in the main of the distribution, but still deviates in the extreme quantiles, as shown in Fig. 5b. Moreover, less than 5 out of the 100 bins are out of the 95% confidence interval on the PIT histogram, which indicates that the predictive distribution is well-calibrated on the training data.

The calibration for the tails can be improved by modelling the tails with a parametric extreme value distribution, resulting in a semi-parametric model. Fig. 5c shows the PIT histogram of a quantile regression model with Generalized Pareto distribution for the 3% upper and lower quantiles applied to the training data. The day-ahead forecast of national demand is used as exogenous variable to model scale and shape parameters of the Generalized Pareto distribution with a thin plate regression spline as smoothing basis [20]. The PIT histogram indicates improvements in terms of calibration compared to the PIT histograms of the other models.

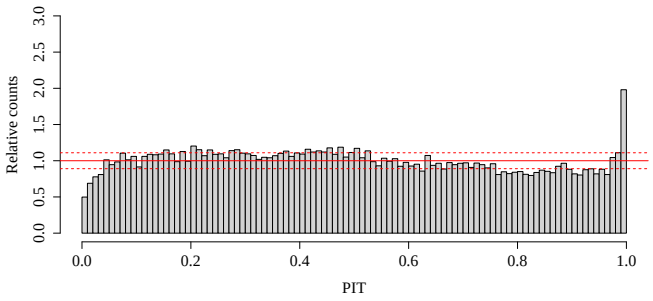


(a) Parametric Gaussian model

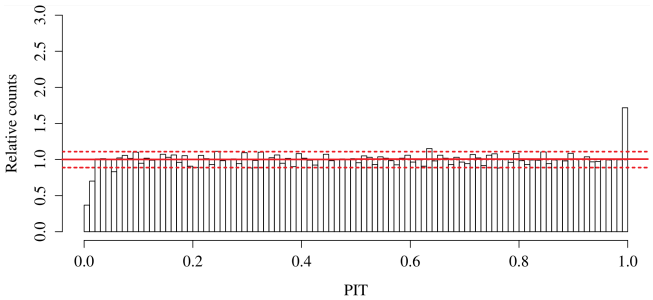


(b) Non-parametric quantile regression model

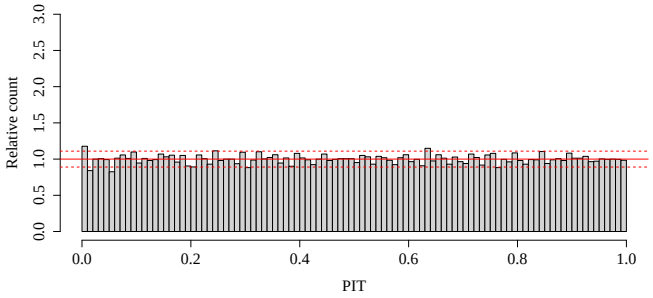


(c) Semi-parametric quantile regression with Generalized Pareto tails

Fig. 5: Histogram of the PIT of the best performing model in Table III applied to the training data.

## V. Validation and Testing of Probabilistic Inertia Forecast Model on Test Data

Although the semi-parametric model is well-calibrated on the training data, it results in unacceptable calibration on the test data. The PIT histogram in Fig. 6 indicates that too many observations in 2018 correspond to the lower quantiles of the predictive distribution. This malfunctioning is caused by slow changes to the GB power system, resulting in bias forecasts. First of all, the coal power plants are phased out over the period from 2016 with significantly reduced output in 2017 and very low output in 2018. Second, the volume of import via interconnectors increases significantly in 2018 compared to 2017 and 2016, especially from October. This evolution causes power plants that provide inertia to be replaced by converter-interfaced import of power. This changes the characteristics of the inertia from transmission-system-connected synchronous generators in the system over time and in relation to available explanatory variables, such as forecasts of electricity demand.

To deal with the changing characteristics of inertia over time, a periodic re-training approach has been applied to the quantile regression and GPD models. The rolling horizon approach fits the forecast models on sliding training windows [21], [27], [28]. The models are updated on a monthly basis and the data of the last month are added to the training set. Data points in the training set are weighted equally the last year plus one month before the forecasting instant, while weights are linearly decreasing for earlier settlement periods. These choices have been made based on the trade off between computational cost and forecast performance. Fig. 7 shows the PIT histogram of the rolling horizon quantile regression model with Generalized Pareto distribution of the tails. The rolling horizon approach improves the calibration of the probabilistic forecast model on the test set compared to

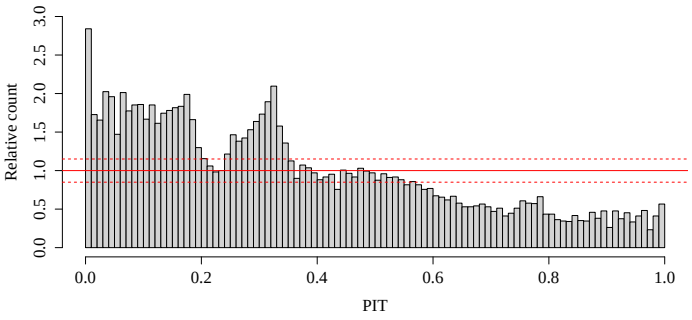


Fig. 6: Histogram of the PIT of the static quantile regression model with Generalized Pareto tails (Semi-parametric) applied to the test data.

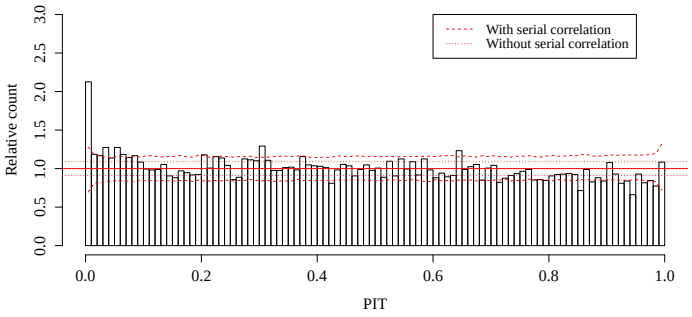


Fig. 7: Histogram of the PIT of the quantile regression forecast model with Generalized Pareto tails (Semi-parametric) and periodic model re-training applied to the test data

the best static probabilistic forecast model, for which the PIT histogram is shown in Fig. 6. This periodic model re-training produces calibrated forecasts and demonstrates the importance of tracking changes in the underlying power system when producing inertia forecasts.

The analysis demonstrates the importance of the developed probabilistic forecast models for system operation. Today, system operation is based on deterministic point forecasts with limited or even naive forecast uncertainty estimation (e.g., Gaussian assumption with constant variance), which are inadequate, especially at low probability levels relevant for risk-based decision making. The PIT histogram of the Gaussian predictive distribution in Fig. 5a shows that using prediction intervals based on the lower quantiles (below 5%), i.e., quantiles representing the most relevant, low-inertia conditions for a risk-averse system operator, are not well-calibrated with the real predictive distribution of inertia. This situation has been improved largely by adopting the semi-parametric model structure, as shown by the PIT histogram in 5c.

Furthermore, the changing nature of power systems necessitates adaptive forecasting methods. A simple solution to this, which borrows from the field of demand and electricity price forecasting as applied in industry, is demonstrated above. While the results show good performance in general, the out-of-sample test suggests that the left tail is not correctly calibrated. This motivates development of more sophisticated adaptive schemes, such as the one in [29], with a specific focus on the extremes/tail distributions, which is the subject of ongoing work.

## VI. Conclusion

The developed probabilistic model is the first explanatory data-driven model to forecast the inertia contribution of transmission-connected synchronous generators in day-ahead, which is furthermore able to accurately quantify uncertainty of inertia forecasts. Accurate uncertainty quantification is crucial to adequately handle the risk of ROCOF and under-frequency relay tripping, and we find the simple approach of assuming a Gaussian predictive distribution to be inadequate. Therefore, semi-parametric density forecasts are produced modeling individual quantiles of the predictive distribution using day-ahead forecasts of national demand, wind and solar power generation, as well as a decreasing trend in the inertia, inertia at the moment of forecasting and interconnector flows, while accounting for the difference between weekdays and weekend days/holidays. To properly model the tails of the predictive distribution, which are crucial to characterize potential low-probability high-impact conditions, the Generalized Pareto distribution has been used. To maintain the calibration of the probabilistic forecasts in power systems with evolving characteristics it is crucial to periodically update forecasting models. Future work will focus on investigating how this forecast model can improve the operational practice for frequency control, which is currently based on point forecasts or approximate interval forecasts. Moreover, other adaptive approaches to track changes in system characteristics should be investigated.

## Acknowledgment

The research of Evelyn Heylen and Fei Teng leading to these results has received funding from Network Innovation Allowance under reference NIA_NGSO0020. Jethro Browell is supported by an EPSRC Innovation Fellowship (EP/R023484/1). We are also thankful to Prof. Georges KARINIOTAKIS and Dr Simon CAMAL at MINES ParisTech for the constructive discussions. Data underlying this article can be accessed on zenodo.org (DOI: 10.5281/zenodo.4708136), and used under the Creative Commons Attribution licence (CC BY).

## References

[1] J. Matevosyan, Implementation of Inertia Monitoring in ERCOT What's It All About?, Accessed 03/11/2020, [Online] Available: https://www.esig.energy/implementation-of-inertia-monitoring-in-ercot-whats-it-all-about/ (2018).

[2] Entso-E, Fast Frequency Reserve Solution to the Nordic inertia challenge.

[3] E. Heylen, G. Strbac, F. Teng, Challenges and opportunities of inertia estimation and forecasting in low-inertia power systems, arXiv preprint arXiv:2008.12692.

[4] P. Du, J. Matevosyan, Forecast System Inertia Condition and Its Impact to Integrate More Renewables, IEEE Transactions on Smart Grid 9 (2) (2018) 1531–1533.

[5] D. Wilson, J. Yu, N. Al-Ashwal, B. Heimisson, V. Terzija, Measuring effective area inertia to determine fast-acting frequency response requirements, International Journal of Electrical Power & Energy Systems 113 (2019) 1–8.

[6] E. Heylen, F. Teng, Inertia forecasting: A system operation perspective, Submitted.
[7] F. Gonzalez-Longatt, M. Acosta, H. Chamorro, D. Topic, Short-term kinetic energy forecast using a structural time series model: Study case of nordic power system, in: 2020 International Conference on Smart Systems and Technologies (SST), IEEE, 2020, pp. 173–178.
[8] J. Browell, M. Fasiolo, Probabilistic forecasting of regional net-load with conditional extremes and gridded nwp, IEEE Transactions on Smart Grid.
[9] C. Gonçalves, L. Cavalcante, M. Brito, R. J. Bessa, J. Gama, Forecasting conditional extreme quantiles for wind energy, Electric Power Systems Research 190 (2021) 106636.
[10] L. Badesa, F. Teng, G. Strbac, Simultaneous scheduling of multiple frequency services in stochastic unit commitment, IEEE Transactions on Power Systems 34 (5) (2019) 3858–3868.
[11] T. Hong, P. Pinson, Y. Wang, R. Weron, D. Yang, H. Zareipour, Energy forecasting: A review and outlook, IEEE Open Access Journal of Power and Energy.
[12] P. Tielens, Operation and control of power systems with low synchronous inertia, PhD Thesis, KU Leuven, Leuven, Belgium (2017).
[13] R. J. Bessa, C. Mhrlen, V. Fundel, M. Siefert, J. Browell, S. Haglund El Gaidi, B.-M. Hodge, U. Cali, G. Kariniotakis, Towards Improved Understanding of the Applicability of Uncertainty Forecasts in the Electric Power Industry, Energies 10 (9) (2017) 1402.
[14] Y. Zhang, J. Wang, X. Wang, Review on probabilistic forecasting of wind power generation, Renewable and Sustainable Energy Reviews 32 (2014) 255–270.
[15] T. Hong, S. Fan, Probabilistic electric load forecasting: A tutorial review, International Journal of Forecasting 32 (3) (2016) 914–938.
[16] J. Nowotarski, R. Weron, Recent advances in electricity price forecasting: A review of probabilistic forecasting, Renewable and Sustainable Energy Reviews 81 (2018) 1548–1568.
[17] T. Hong, P. Pinson, S. Fan, H. Zareipour, A. Troccoli, R. J. Hyndman, Probabilistic energy forecasting: Global Energy Forecasting Competition 2014 and beyond, International Journal of Forecasting 32 (3) (2016) 896–913.
[18] R. Koenker, Quantile Regression, Econometric Society Monographs, Cambridge University Press, 2005.
[19] J. Beirlant, Y. Goegebeur, J. Segers, J. L. Teugels, Statistics of extremes: theory and applications, John Wiley & Sons, 2006.
[20] S. N. Wood, N. Pya, B. Säfken, Smoothing parameter and model selection for general smooth models, Journal of the American Statistical Association 111 (516) (2016) 1548–1563.
[21] T. Gneiting, K. Larson, K. Westrick, M. G. Genton, E. Aldrich, Calibrated probabilistic forecasting at the stateline wind energy center: The regime-switching space–time method, Journal of the American Statistical Association 101 (475) (2006) 968–979.
[22] F. Laio, S. Tamea, Verication tools for probabilistic forecasts of continuous hydrological variables, Hydrol. Earth Syst. Sci. (2007) 11.
[23] P. Pinson, P. McSharry, H. Madsen, Reliability diagrams for non-parametric density forecasts of continuous variables: Accounting for serial correlation, Quarterly Journal of the Royal Meteorological Society 136 (646) (2010) 77–90.
[24] H. Hersbach, Decomposition of the Continuous Ranked Probability Score for Ensemble Prediction Systems, WEATHER AND FORECASTING 15 (2000) 12.
[25] A. Fernndez-Guillamn, E. Gmez-Lzaro, E. Muljadi, A. Molina-Garca, Power systems with high renewable energy sources: A review of inertia and frequency control strategies over time, Renewable and Sustainable Energy Reviews 115 (2019) 109369.
[26] R. Koenker, G. Bassett, Regression quantiles, Econometrica 46 (1) (1978) 33–50.
[27] A. S. Hering, M. G. Genton, Powering up with space-time wind forecasting, Journal of the American Statistical Association 105 (489) (2010) 92–104.
[28] J. Dowell, P. Pinson, Very-short-term probabilistic wind power forecasts by sparse vector autoregression, IEEE Transactions on Smart Grid 7 (2) (2015) 763–770.
[29] D. Obst, J. de Vilmarest, Y. Goude, Adaptive methods for short-term electricity load forecasting during covid-19 lockdown in France, arXiv preprint arXiv:2009.06527.

## APPENDIX

TABLE IV: Coefficients of the forecast models in Eq. (5) and Eq. (6)

| | Eq. (5) | Eq. (6) free days | Eq. (6) non-free days |
|---|---|---|---|
| $E_t^{I,G}$ | 0.154 | 6.44E-02 | 0.149 |
| $\hat{P}_t^{ND}$ | 3.495 | 3.513 | 3.204 |
| $\hat{P}_t^{wind}$ | -2.915 | -3.001 | -3.128 |
| $\hat{P}_t^{solar}$ | -0.767 | -0.738 | -0.305 |
| $t$ | 6.58E-05 | 1.73E-04 | 1.73E-04 |
| $t^2$ | -2.15E-04 | -6.91E-04 | -6.91E-04 |
| $P^{ic}$ | NA | -3.325 | -4.29 |